16th Australasian Fluid Mechanics Conference
Crown Plaza, Gold Coast, Australia
2-7 December 2007

# Strain-rate development between a co-rotating Lamb-Oseen vortex pair of unequal strength.

**Hannah Busch[1], Kris Ryan[1] & Gregory J. Sheard[1,2]**

[1]Fluids Laboratory for Aeronautical and Industrial Research (FLAIR), Department of Mechanical Engineering
Monash University, VIC, 3800, Australia.

[2]Monash University Biomedical Engineering Technology Alliance (MuBeta)
Monash University, VIC 3800, Australia

## Abstract

To date, several investigations have considered the prospect of enhanced dissipation of a vortex pair due to elliptic (short wave) instabilities. Recent studies indicate that these modes have the potential to significantly reduce the time taken to dissipate vortex pairs. This has generated interest in the aviation industry, where aircraft trailing wakes pose a significant hazard for nearby aircraft.

Of note, recent studies have indicated that the growth rate of these short-wave instability modes depends strongly on the strain-rate developed within the core of each vortex. This strain-rate has been shown to develop naturally simply due to the presence of both vortices.

Studies to date have concentrated on vortex pairs where each vortex has the same magnitude of circulation. We extend this by varying the circulation ratio of the two vortices; the circulation of one vortex is varied while the circulation of the other remains constant. The effect on the strain-rate which develops within each core is considered. Of particular interest are the time-scales involved in both the strain-rate development and in the two-dimensional merging process, as sufficient time is required for short-wavelength instabilities to occur prior to merging for the process to successfully reduce dissipation time.

A spectral-element method is used to conduct the DNS investigation at a circulation Reynolds number of $Re_\Gamma$ = 20,000.

## Introduction

A significant problem facing the aviation industry today is the danger imposed by large commercial aircraft trailing wakes. The wake region of an aircraft is highly turbulent and contains a counter rotating vortex pair that remains coherent for a long time (Gerz, Holzäpfel & Darracq 2002). This poses a significant hazard to trailing aircraft; a loss of control may occur when entering a wake of another aircraft and a number of accidents and near misses have been recorded (FAA Wake Turbulence Training Aid, 2007).

Co-rotating vortices develop with circulation of the same sign; an example of this is a wing-tip / wing-flap pair. As they travel downstream of generation, they interact and a merging process takes place. This merger results in a single vortex that, due to symmetry about the centreline of an aircraft, becomes one half of a counter-rotating vortex pair of a trailing wake.

Figure 1 illustrates the parameters of a co-rotating vortex pair that will be discussed throughout this paper. The effective vortex radius is defined as *a*, the separation between the cores as *b*, and the circulations as $\Gamma_1$ and $\Gamma_2$ respectively.

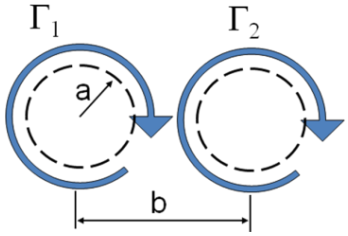


Figure 1 : 2D representation of co-rotating parallel vortices. Here *a* is the characteristic vortex radius, *b* is the separation distance between the vortex cores and the vortex circulations as $\Gamma_1$ and $\Gamma_2$ respectively.

One of the key parameters in this field of research is the Reynolds number based on the circulation of a vortex. This is defined as the ratio between circulation and the viscous forces:

$$Re_\Gamma = \frac{\Gamma}{\nu}\,, \tag{1}$$

where $\nu$ is the kinematic viscosity of the fluid.

A number of parameters have been studied extensively regarding the merging process including circulation Reynolds number, vortex strength, separation between the cores of the vortices and vortex radius. It has been determined experimentally by Meunier & Leweke (2001) that for equal-circulation equal-strength co-rotating vortices, a critical value of separation ratio exits as $\left(\frac{a}{b}\right)_c = 0.29 \pm 0.01$. Below this value merging will not occur under the inviscid conditions. When viscous effects are taken into account, a diffusive stage exists where the vortex radii grow until $\left(\frac{a}{b}\right) = \left(\frac{a}{b}\right)_c$ which marks the start of the merging process (Meunier & Leweke 2001). The radial growth rate has been shown to occur according to

$$a(t) = \sqrt{a_0^2 + 4\nu t}\,, \tag{2}$$

where $a_0$ is the initial vortex radius, $\nu$ is the fluid viscosity and *t* is the current time.

A key feature of interacting vortices is the growth of three-dimensional instabilities. Crow (1970) first described a long-wave instability mode growing within the trailing vortices of aircraft. It develops sinusoidally within counter-rotating vortex pairs, forming vortex rings which rapidly dissipate. The Crow instability has a relatively slow growth rate enabling vortices to remain coherent for extended periods.

Jimenez (1975) analytically determined that co-rotating vortex pairs would be stable to this Crow instability and Meunier & Leweke (2005) confirmed this, noting that there was no long-wave instability observed when they experimentally studied a co-rotating vortex pair. In an experimental study by Leweke & Williamson (1998) on counter-rotating vortices, a shorter wavelength instability was observed to occur concurrently with the Crow instability. They found it to significantly increase the normalized instability growth rate σ*, and identified this short-wave instability to be an elliptical instability, in which the vortex core streamlines are elliptically deformed. Meunier & Leweke (2005) found that, for a co-rotating Lamb-Oseen vortex pair, the presence of elliptical instabilities resulted in an earlier onset of the merging process than corresponding two-dimensional models for $Re_\Gamma > 2000$. It was proposed that these instabilities lead to a quick growth of $a/b$ hence aiding the merging process.

In Kerswell's (2002) review of elliptical instability he remarks that the growth rate of three-dimensional elliptical instabilities scale with strain-rate. A number of other studies state that the elliptical deformations, which lead to elliptical instabilities, develop as a result of mutually induced strain (Le Dizès & Laporte 2002, Leweke & Williamson 1998). Le Dizès & Verga (2002) found two-dimensional co-rotating vortices elliptically deform identically on a non-viscous time scale for $500 \leq Re_\Gamma \leq 16{,}000$, demonstrating a link between the flow Reynolds number and the underlying strain field.

However, to date there has not been any emphasis placed on how the strain-rate develops within a Lamb-Oseen vortex pair when considering a vortex pair of unequal circulation (i.e. for $\Lambda = \Gamma_1/\Gamma_2 \neq 1$). The simulations reported here demonstrate the relationship between the ratio of circulations and the vortex core strain-rate for unequal co-rotating vortices.

## Flow Geometry

When analysing vortex pair interactions, prior studies have considered a number of different vortex profiles. In particular, researchers have considered Batchelor, Lamb-Oseen and Rankine profiles. The simplest of these is the Rankine profile, consisting of uniform vorticity out to the maximum vortex radius (Treiling, Fuentes & van Heijst 2005).

Meunier & Leweke (2001) found experimentally that an initial vortex profile was of Gaussian type, and Le Dizès & Verga (2002) numerically demonstrated that any two dimensional axisymmetric vortex will relax towards a Gaussian profile. A Gaussian profile has a peak vorticity at the core which exponentially decreases outwards. A Gaussian type vortex profile is represented by,

$$\omega_0 = \frac{\Gamma}{\pi a_0^2} e^{-r^2/a_0^2} \ , \tag{3}$$

where $r$ is the radial distance from the centre and $a_o$ is the initial vortex radius. This particular profile is known as the Lamb-Oseen vortex (Le Dizès & Verga 2002).

Our study considers a Lamb-Oseen vortex pair, and initially both vortices have the profile described by equation 3. However, unlike prior studies, we consider the case where each vortex within the pair has a different circulation. In order to do this, we define the circulation ratio as

$$\Lambda = \frac{\Gamma_1}{\Gamma_2} \ , \tag{4}$$

where $\Gamma_2$ is the circulation of the dominant vortex, and $\Gamma_1$ is the circulation of the weaker vortex. To the authors' knowledge, prior studies have only considered $|\Lambda| = 1$.

In order to compare results with prior investigations, a non-viscous time scale is being used, defined as

$$t^* = \frac{t\Gamma}{2\pi a_0^2} \ . \tag{5}$$

Here, $\Gamma$ is the circulation of the dominant vortex and $a_0$ is the initial radius of the dominant vortex.

To ensure that the results obtained are meaningful, a comparison with the findings of Le Dizès & Verga (2002) was made. In their studies they investigated equal strength co-rotating vortex pairs for vortices with a variety of profiles. They noted that the addition of two identical Gaussian vortices was not a solution of the Navier-Stokes equations. A 'relaxation' period was described during which the vortices adjust to form an elliptic profile. After this adjustment period (which was found to be inviscid) the two vortices diffuse, gradually increasing their aspect ratio prior to merging. They found that the Gaussian profile was a global attractor of any two-dimensional axisymmetric vortex; the more Gaussian-like the initial profile, the quicker the relaxation period.

The variable used by Le Dizès & Verga (2002) to describe the temporal change in vortex profile over the relaxation period was the eccentricity of the vortex profile, ε. They noted that the eccentricity was a function of the strain field which one vortex imposed on the other, defining the eccentricity as

$$\varepsilon = \frac{S_i}{1/2\,\omega_z} \ . \tag{6}$$

Here, $S_i$ is the internal strain-rate (defined as the strain measured at the vortex core imposed from both vortices) and $\omega_z$ is the vorticity measured at the core. Although Le Dizès & Verga (2002) investigated flow Reynolds numbers between $500 \leq Re_\Gamma \leq 16000$, they found only a weak dependence on Reynolds number.

## Numerical Technique

The direct numerical simulations of the governing fluid equations were completed using a spectral-element method. The technique is 3rd order accurate in time and has been successfully used in several prior studies (e.g. Sheard et al 2007).

For this study the circulation Reynolds number of the dominant vortex is being limited to $Re_\Gamma = 20{,}000$ for two reasons. The first being that at low Reynolds numbers, viscous effects become significant and cannot be neglected. A previous study by Le Dizès and Verga (2002) showed that within the Reynolds numbers $800 \leq Re_\Gamma \leq 8000$, merging of co-rotating vortices will always occur due to the viscous diffusion of vorticity. The value chosen for this study is sufficiently high to minimise this viscous diffusion. It also is sufficiently low that a turbulent flow regime will not develop. Spectral-element methods are best suited to smooth solutions (Karniadakis & Sherwin 2005), so turbulence is an undesirable flow regime. Turbulence modelling is also computationally expensive; to capture the fine flow structures, a very refined mesh is required which increases computational time beyond what is suitable for a study of this scale.

At this Reynolds number, the circulation ratio Λ has been varied between $0.1 \leq \Lambda \leq 1.0$ in increments of 0.1. The initial separation ratio has been set at $(a/b)_0 = 0.15$ to delay the merging process, allowing for an extended period in which the vortex core strain-rate can be observed.

## Results

Here, we consider the strain-rate development for both vortices as a function of reduced time, $t^*$. The results are subdivided to consider the dominant vortex and the weaker vortex separately.

### Dominant vortex results

Figure 2 shows the time evolution of the strain-rate $S$ for the dominant vortex at various values of $\Lambda$. Here the strain-rate has been calculated within the core of the vortex, and includes the effects of both the internal and external strain fields.

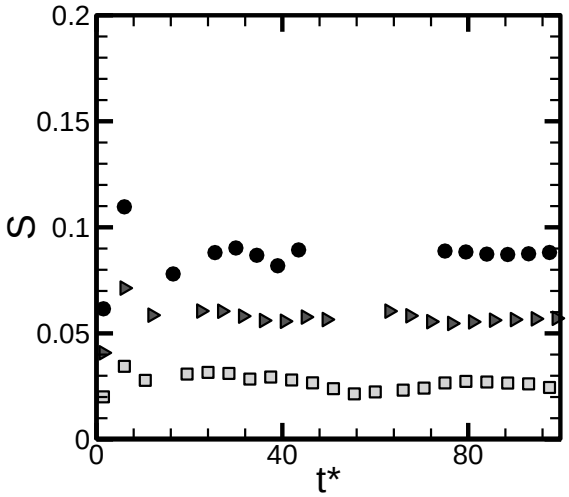


Figure 2 : Time evolution of the core strain-rate $S$ for the dominant vortex for different ratios of circulation. Shown are $\Lambda$ = 0.3 (squares), $\Lambda$ = 0.6 (triangles) and $\Lambda$ = 0.9 (circles). The relaxation period ends at $t^* \approx 40$ for all $\Lambda$ considered.

For each value of $\Lambda$, an initial increase in $S$ is observed, prior to a sudden decrease in value. An oscillation in $S$ over time is noted, until a steady-state condition is reached. The steady-state value of $S$ is reached after approximately 40 normalized time units regardless of circulation ratio. However small oscillations are observed around a median value at later times.

This weak fluctuation can be seen throughout vorticity profiles as well. Figure 3 pictorially shows the effect of the relaxation period. The periodic change in direction of eccentricity is due to the weaker vortex encircling the dominant one. At the commencement of the simulation (Figure 3a) the weaker vortex is to the left of the dominant vortex. At the conclusion of the simulation, the weaker vortex is to the right of the dominant vortex (Figure 3h). The position of the weaker vortex is made apparent in figure 3 by following the major axis direction of the dominant vortex.

Referring back to Figure 2, the value of strain-rate is clearly affected by the value of $\Lambda$; this is not surprising, as $|\Lambda| \to 0$, the weaker vortex has less influence on the dominant vortex and the strain-rate within the dominant vortex $S \to 0$. Our results confirm this conclusion.

Analysing the data outside the inviscid relaxation period (i.e. for $t^* > 40$) we note that the strain-rate of the dominant vortex gradually increases over time. This is due to viscous diffusion which acts to increase the major axis of the vortex faster than the minor axis. Using a linear least squares fit, the increase in strain-rate may be modelled. Two important pieces of information come from this model. First, we may extrapolate back to $t^* = 0$, to find an 'initial' strain-rate. This strain-rate is not observed numerically, however it allows us to compare the variation in $S$ magnitude as a function of $\Lambda$. Second, the gradient of the line provides a measure of strain-rate growth, which is also observed to alter as a function of $\Lambda$.

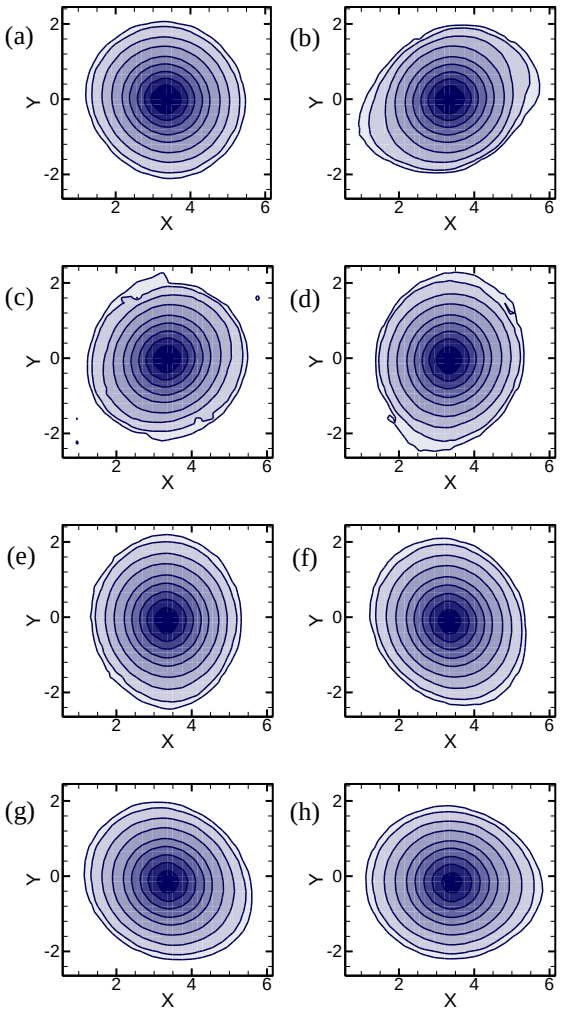


Figure 3 : Contours of vorticity throughout the relaxation period of the dominant vortex in the case $\Lambda$ = 0.9. (a) represents the initial vortex profile, (b) – (h) represent $10 \le t^* \le 70$ in increments of $\delta t^* = 10$. Of particular interest is the vorticity contours of (a)-(d) which are within the relaxation period.

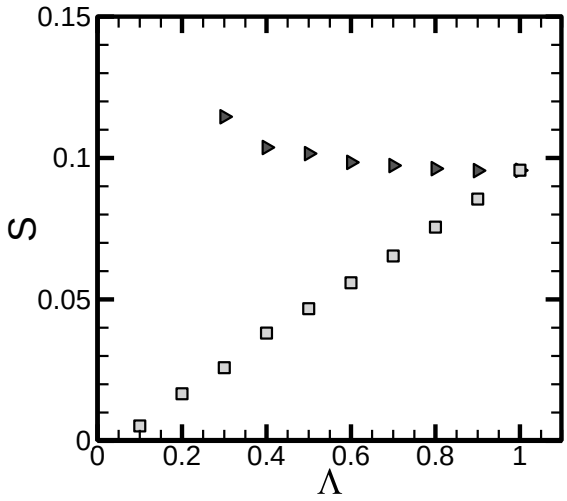


Figure 4 : Estimated strain-rate at $t^* = 0$ at the vortex core. Dominant vortex (squares), secondary vortex (triangles). The increasing $S_i$ of the dominant vortex is indicative of the increasing strength of the secondary vortex. The decreasing $S_i$ of the secondary vortex is indicative of the decrease in relative strength of the dominant vortex.

Figure 4 shows the calculated, 'initial' strain-rate of the dominant and weaker vortices as a function of Λ. From the figure, it is seen that the 'initial' core strain-rate of the dominant vortex has a linear dependence on the strength of the weaker vortex. As Λ→ 1, the strain-rate in the stronger vortex becomes more pronounced. This is expected; as Λ increases, the weaker vortex has a more dominating effect on the flow field, causing a stronger response from the dominant vortex.

The gradient determined from the data shown in Figure 2 has a different trend to that of the initial values throughout the various values of Λ. Figure 5 shows these gradients as a function of Λ.

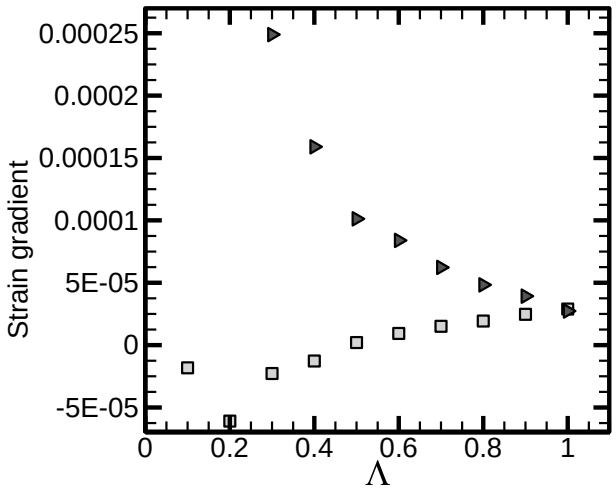


Figure 5 : Estimated strain-rate gradient at the vortex core according to the non-viscous time evolution of strain-rate. For comparison is the dominant vortex (squares) and the secondary vortex (triangles).

For circulation ratios of Λ = 0.5 or above, it can be seen that until $t^*$=100, the strain-rate progressively increases at the core of the dominant vortex. For values below Λ = 0.5, it appears that the core strain-rate decreases with time.

For Λ = 0.1, it can be deduced that the initial strain-rate is not large enough to produce a prolonged strain-rate decrease, hence the gradient is quite low. For Λ = 0.2 there is a rapid loss of vorticity experienced by the weaker vortex and the induced strain of approximately $S$ = 0.02 is not maintained for a long time. As the weaker vortex dissapates to below ω = 0.1 there is a rapid decrease in the dominant vortex strain-rate as the system "relaxes" to only having one vortex present. For Λ = 0.3, the weaker vortex remains coherent for the entire span of $t^*$. Its vorticity weakens to a level much lower than the Λ = 0.4 case, and hence has less of an impact on the dominant vortex. This reduced impact allows the dominant vortex to more readily absorb the induced strain, and relax to the strain-rate. The case of Λ = 0.5 demonstrates that the induced strain-rate at the dominant vortex core reaches almost an equilibrium situation, where very little change in strain-rate is observed. At circulation ratios greater than Λ = 0.5, the strain induced strain-rate increases as the simulations proceed.

**Weaker vortex results:**

As per the dominant vortex, the analysis of the secondary vortex is undertaken by first scaling the results to a non-viscous time scale. Figure 6 shows the strain-rate as a function of $t^*$.

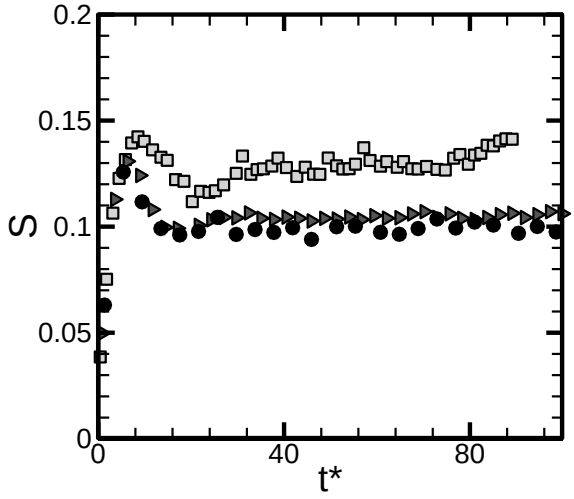


Figure 6 : Time evolution of the strain-rate $S$ for the weaker vortex at values of Λ = 0.3 (squares), 0.6 (triangles) and 0.9 (circles). All three vortex profiles again are subject to a relaxation period, $t^* < 40$.

For the purpose of the following discussion, the plots of Λ = 0.1 and 0.2 have been omitted, and will be discussed later in this paper. Again the trend for the results is a weak oscillation up to approximately $t^*$ = 40, where beyond this value, stability of the solution is achieved. To further quantify these results, the approximated $t^*$ = 0, 'initial' strain-rate and the gradient of these strain-rate curves are also shown in Figure 4 and Figure 5 respectively.

As opposed to the increasing initial strain-rate values for the dominant vortex, Figure 4 shows the estimated 'initial' core strain-rate decreasing as the strength of the vortex increases. Intuitively, this is to be expected as the relative vorticity of the dominant vortex is lessened. This initial strain-rate decreases asymptoticaly to the equal strength condition where Λ = 1.0.

Also opposing the trends seen in the dominant vortex strain-rate plots, the gradient of the strain-rate curves beyond $t^*$ = 40 shows a decreasing trend.

Re-including the strain-rate plots of Λ = 0.1 and 0.2 as Figure 7, it can be quickly seen that their behaviour is markedly different to that of the other circulation ratios.

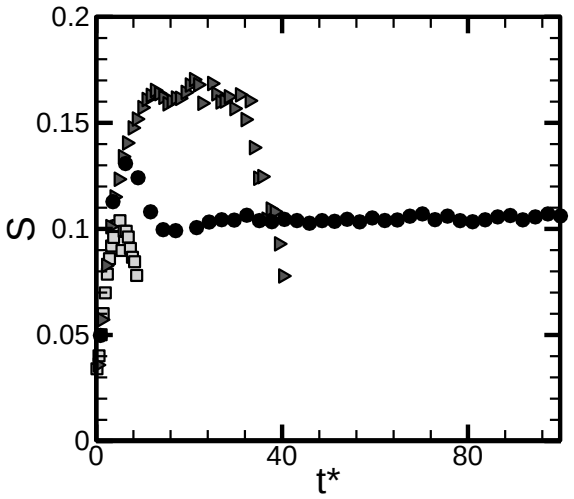


Figure 7 : Strain-rate of the two weakest vortices, $\Lambda$ = 0.1 (square), 0.2 (triangles) and 0.6 (circles). Illustrated is the inconsistent vortex strain-rate behaviour once the vorticity drops below $\omega$ = 0.1 in comparison to the coherent secondary vortex of the $\Lambda$ = 0.6 case.

The peak strain-rate for $\Lambda = 0.2$ is far higher than any other of the vortices modelled, a comparative graph of $\Lambda = 0.6$ illustrates this. For these low strength secondary vortices, it may be that the decrease in vorticity below the $\omega = 0.1$ represents a threshold for vortex dissipation ($\omega = 0.1$ was used a cut-off minimum value when tracking the vortex cores). Further investigations into this area would be needed to fully conclude their behaviour.

## Conclusions

The prior studies of co-rotating vortices have until now have focused on equal strength pairs or not investigated vortex core strain-rate. This paper demonstrates the behaviour of both the dominant and secondary vortex in a vortex pair, in terms of core strain-rate. It has been verified that a relaxation period exists for the numerical simulation of a co-rotating vortex pair, and that stability occurs beyond $t^* = 40$ on non-viscous time scale. Analysing the available data beyond this point reveals that the strain-rate in both the dominant and secondary vortices develops linearly. For circulation ratios of $\Lambda = 0.4$ and below, the dominant vortex experiences a decrease in core strain-rate, attributed to the low strength of the weaker vortex. $\Lambda = 0.5$ and beyond sees the dominant vortex core strain-rate increasing with time.

The weaker vortex behaves similarly, responding to the relative magnitude of the dominant vortex. As the strength of the weaker vortex increases, the initial core strain-rate decreases and the rate at which the strain-rate increases, is reduced. The two cases of $\Lambda = 0.1$ and 0.2 indicate that the weaker vortex may become incoherent when it's vorticity reduces to below $\omega = 0.1$. This may form the basis of further studies.

## Acknowledgements

The authors would like to acknowledge the strong support from the Australian Partnership for Advanced Computing (APAC) which enabled this research to take place.

## References

[1] Crow, S., Stability theory for a pair of trailing vortices, *AIAA Journal*, **V8**, 1970

[2] Gerz, T., Holzäpfel, F., Darracq, D., Commercial aircraft wake vortices, *Progress in Aerospace Sciences*, **V38**, 2002, 181-208

[3] Jimenez, J., Stability of a pair of co-rotating vortices, *Physics of Fluids*, **V18**, 1975

[4] Karniadakis, G. E. & Sherwin, S. *Spectral/hp element methods for computational fluid dynamics*, Oxford University Press, 2005

[5] Kerswell, R., Elliptical Instability, *Annual Review of Fluid Mechanics*, **V34**, 2002

[6] Le Dizès, S. & Laporte, F., Theoretical predictions for the elliptical instability in a two-vortex flow, *Journal of Fluid Mech*, **V471**, 2002

[7] Le Dizès, S. & Verga, A., Viscous interactions of two co-rotating vortices before merging, *Journal of Fluid Mechanics*, **V467**, 2002

[8] Leweke, T. & Williamson, C., Cooperative elliptic instability of a vortex pair, *Journal of Fluid Mech*, **V360,** 1998

[9] Meunier, P. & Leweke, T., Three dimensional instability during vortex merging, *Physics of Fluids*, **V13**, 2001, pp 2747-2750

[10] Meunier, P. & Leweke, T., Elliptic instability of a co-rotating vortex pair, *Journal of Fluid Mech*, **V533,** 2005

[11] Sheard, G. J., Leweke, T., Thompson, M. C. & Hourigan, K., The effect of mass ratio and tether length on the flow around a tethered cylinder, *Journal of Fluid Mechanics*, 2007

[12] Treiling, R. R, Velasco Fuentes, O. U. & van Heijst, G. J. F., Interaction of two unequal corotating vortices, *Physics of Fluids*, **V17**, 2005

**Internet Sources**

FAA Wake Turbulence Training Aid, Pilot and Air Traffic Controller guide to wake turbulence, 20-June-1995, accessed 30-May-2007

http://www.faa.gov/education_research/training/media/wake/04SEC2.PDF

.